RUTHENIUM-BASED DSSC EFFICIENCY OPTIMIZATION BY GRAPHENE QUANTUM DOT DOPING

Ana Bărar[1] and Doina Mănăilă-Maximean[2]

This paper presents a novel method for ruthenium-based dye-sensitized solar cell (DSSC) power-conversion efficiency optimization, which consists of TiO_2 active layer sensitization with graphene quantum dots. Under proper excitation illumination, graphene quantum-dots emit photons of wavelengths which are absorbed by the ruthenium molecules in the active layer, thus enhancing free electron generation in the DSSC structure. A power-conversion efficiency of 11.27%*, under halogen lamp illumination, is reported for ruthenium-based DSSC samples doped with graphene quantum-dots. This result represents a difference of* 9.57%*, compared to a reference ruthenium-based DSSC sample with* 1.70% *power-conversion efficiency, under halogen lamp illumination.*

Keywords: solar cell, dye-sensitized solar cell, graphene quantum-dots, photovoltaic effect

1. Introduction

Dye-sensitized solar cells (DSSC) have been investigated as an alternative to inorganic photovoltaic devices, due to their simple and cost-effective fabrication method [1], environmental-friendly materials [2,3], and good performance under diffuse light conditions [4]. Several theoretical and experimental studies have been carried out concerning DSSC behaviour in extreme conditions, such as high temperature [5–7], in order to assess and optimize device performance. Other approaches to device power-conversion efficiency optimization consisted of novel dye synthetisation [8–13]. Ruthenium complexes are frequently used in DSSC photosensitization, due to their long excited-state lifetime and high electrochemical stability [14–16]. Among these compounds, $di-tetrabutylammonium\ cis-bis(isothiocyanato)bis(2,2'-bipyridyl-4,4'-dicarboxylato)ruthenium(II)$ (N719) is particularly popular, due to its remarkable efficiency as a photosensitizer [17]. Previous studies on inorganic composites subjected to electromagnetic fields have yielded promising results in the control of the phase and polarization of the reflected and transmitted light [18, 19], coherent control of the scattered optical field by using electrically- and magnetically-responsive colloids [20–22], and even the possibility of achieving quantum effects in certain structures [23]. All these results can be successfully combined with the DSSC manufacturing techniques in order to provide qualitatively-superior devices in terms of light concentration, polarization control and guiding within the DSSC structure, and even nonlinear conversion through desired magnetically-driven techniques.

[1]Lecturer, Department of Electronic Technology and Reliability, University POLITEHNICA of Bucharest, Romania, e-mail: ana.barar@upb.ro

[2]Professor, Physics Department, Faculty of Applied Sciences, University POLITEHNICA of Bucharest, 060042, Bucharest, Romania

This work focuses on N719 dye enhancement with graphene quantum-dot (GQD) doping, for DSSC performance optimization. The N719 dye absorption spectrum is shown in Figure 1, where three absorption maxima are outlined: 313 nm, 390 nm and 512 nm, respectively. By doping a N719-based DSSC sample with GQD particles, small photon emitters are inserted in the proximity of the dye molecules, which, under proper illumination (200-350 nm) [24, 25], will generate 400-500 nm photons close to ruthenium molecules, where they will be easily absorbed, therefore contributing to free electron generation within the active layer of the device, and further exploiting the 390 nm absorption peak of N719.

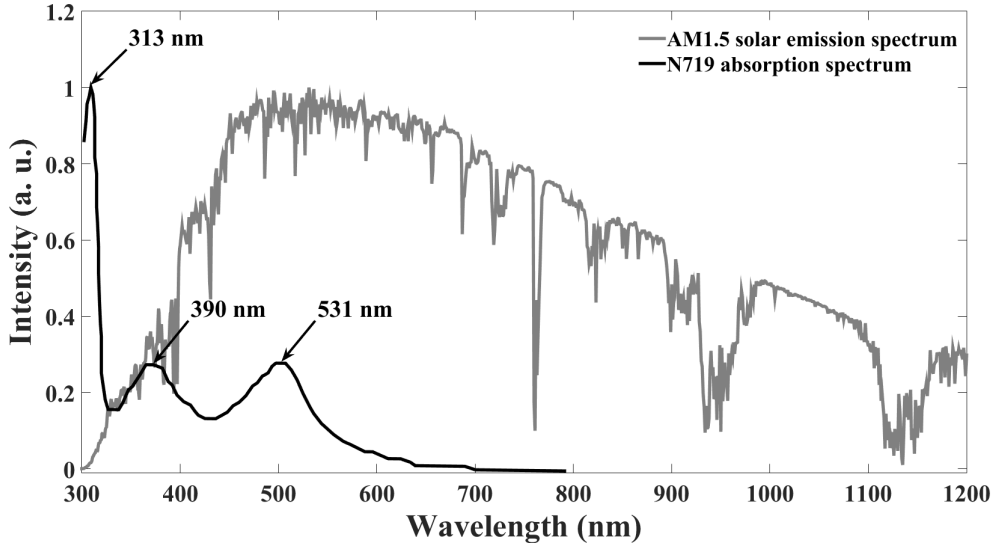

Fig.1. Cross-reference between the AM1.5 solar emission spectrum [26] and ruthenium (N719) absorption spectrum [27, 28]

The work reported in this paper is an experimental demonstration of a theoretical model presented in [29]. This model consists of a simulated DSSC structure, photosensitized with N719, and doped with a variable concentration of GQD particles. The simulation yields the structure's incident photon-to-current conversion efficiency (IPCE) as a function of GQD particle concentration (C_{QD}), where IPCE is defined as:

$$IPCE(\lambda) = LHE(\lambda) \cdot \Phi_{inj} \cdot \eta_{coll} \tag{1}$$

where $LHE(\lambda)$ is the light harvesting efficiency of the dye, Φ_{inj} is the quantum of electron injection from the excited dye molecules into the TiO_2 layer, and η_{coll} is the electron collection efficiency of the electrode from the TiO_2 layer. The simulated data shown in Figure 2 demonstrates an increase in photon-to-current conversion efficiency (IPCE), with an increase in GQD concentration, compared to IPCE values obtained for the DSSC structure untreated with GQD particles.

This paper reports a 11.27% power-conversion efficiency, under halogen lamp illumination, for ruthenium-based DSSC samples doped with graphene quantum-dots. This result represents a difference of 9.57% , compared to a reference N719-based DSSC sample with a 1.70% power-conversion efficiency, under halogen lamp illumination.

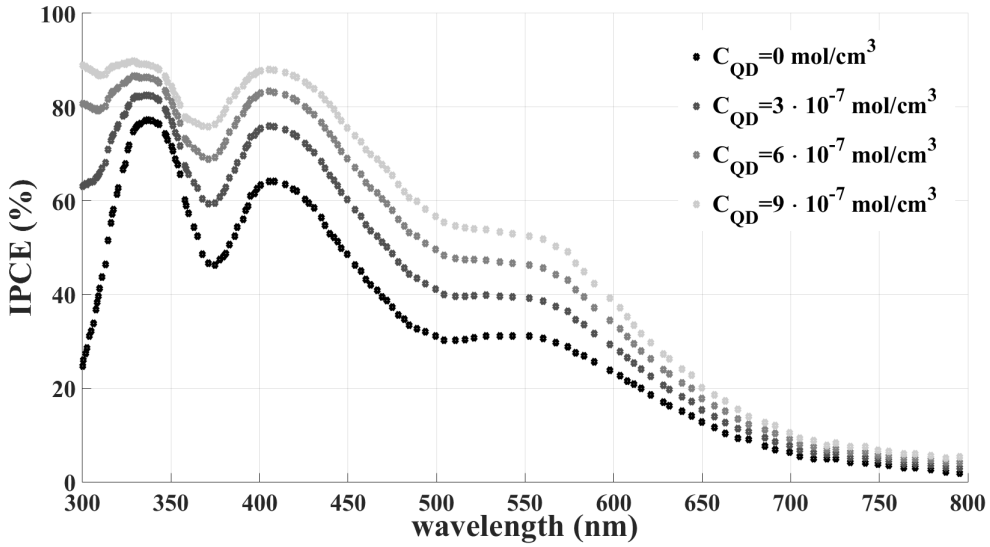

Fig. 2. IPCE of the simulated DSSC structure, for different graphene quantum-dot concentrations [29]

2. **Fabrication method**

The DSSC samples reported in this paper follow the standard architecture [4,14], with the TiO_2 being photosensitized with a N719-based dye containing graphene quantum-dot suspensions, which emit photons of 445 nm wavelength, under 350 nm excitation. Graphene quantum dots were extracted from an aqueous solution with 1 mg/ml concentration (purchased from Sigma-Aldrich), through evaporation at $70°C$, for 24 hours, and suspended in 2 ml ethanol. The fluorescence of GQDs suspended in ethanol was verified under ultraviolet illumination, as shown in Figure 3. Ruthenium N719 powder (Solaronix Ruthenizer 535-bisTBA) was mixed with ethanol and the GQD solution. Ready-made TiO_2 cathodes (purchased from Solaronix) were photosensitized by being immersed for 5 hours in the mixture. Once the the photosensitization step is complete, the cathode is cleaned of excess solution with ethanol, and dried at $40°C$, for 15 minutes. Ready-made platinum anodes (purchased from Solaronix) were sintered at $300°C$ for 45 minutes, in order to eliminate impurities, and the DSSC samples were assembled and filled with an iodide/triiodide electrolytic solution (Solaronix Iodolyte AN-50), by following the standard procedure [4, 30]. For this work, two cathodes were photosensitized with mixtures containing 0.5 mg GQD (QD0.5B),and 1 mg GQD (QD1B), respectively. An additional reference sample was photosensitized using a simple ruthenium N719 dye solution, with no added GQD, and assembled according to the standard procedure. The photosensitization and sample assembly steps, as well as the resulting DSSC samples are presented in Figure 4.

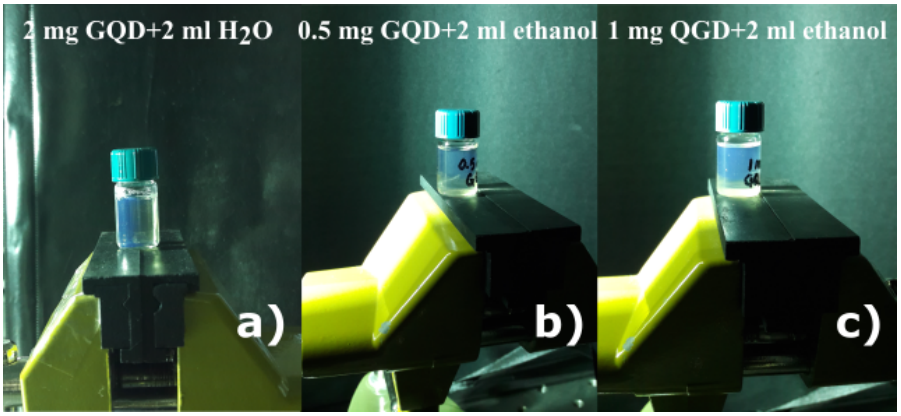

Fig. 3. Fluorescence emitted graphene quantum dot solutions, where a) 1 ml water with 1 mg of GQD suspensions, b) 2 ml ethanol with 0.5 mg GQD suspensions, and c) 2 ml ethanol with 1 mg GQD suspensions

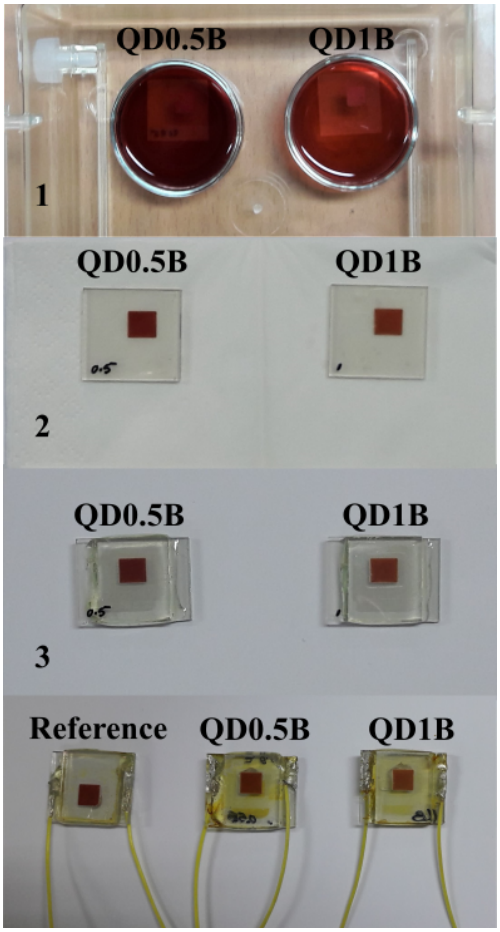

Fig. 4. DSSC sample fabrication steps, where 1 - QD0.5B and QD1B cathodes after photosensitization, 2 - QD0.5B and QD1B electrode assembly, after N719 photosensitization

3. Experimental characterization

The experimental current-voltage (IV) and power-voltage (PV) characteristics of the resulting DSSC samples are measured using a standard setup, where a halogen lamp was used as a light source. The emission spectrum of the halogen lamp is presented in Figure 5.

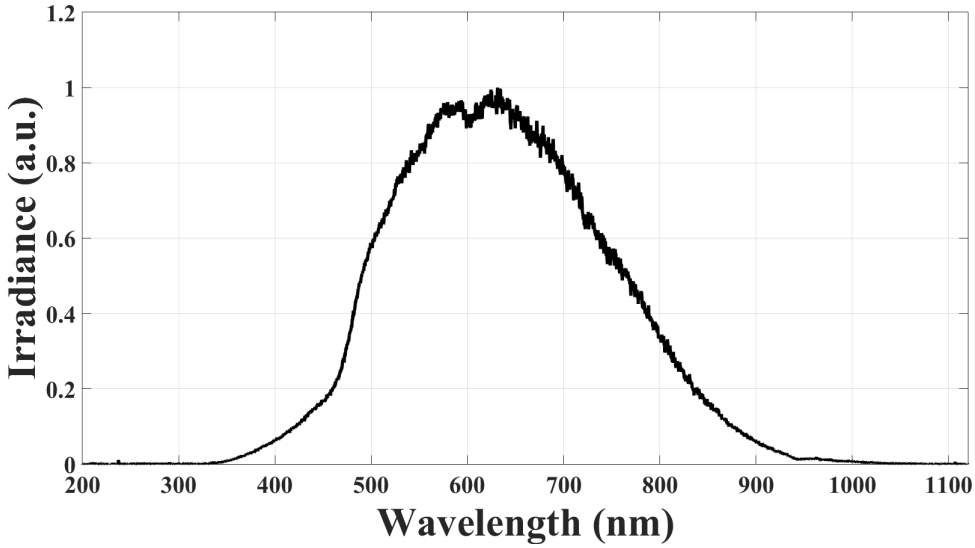

Fig. 5. Emission spectra of the halogen lamp used as light source in the experimental setup for DSSC sample characterization

DSSC samples internal parameter values were extracted from the experimental IV curve, using an algorithm we developed in earlier work [31,32], which involves the asymptotic approximation method, followed by the W Lambert function [33,34]. The main device internal parameters extracted are: open-circuit voltage, short-circuit current, cell shunt resistance, cell series resistance, cell ideality factor, P_{max} - cell maximum power yield, fill-factor, and power-conversion efficiency.

4. Results and discussions

The experimental IV and PV curves obtained for DSSC samples QD0.5B and QD1B, as well as the reference sample, are shown in Figure 6, and the device parameters extracted from the experimental curves for all three samples are presented in Table 1.

The numerical values of device parameters obtained for the GQD doped samples indicate a substantial performance improvement, compared to the reference sample. For 1 mg GQD sample doping, open-circuit voltage is increased with $100\,mV$, compared to the reference value, and the short-circuit current increases to $50\,\mu A$. The shunt resistance is increased by an order of magnitude for an added 1 mg of GQD, which indicates that GQD particles do not create bulk defects within the TiO_2 layer. The series resistance remains to the same order of magnitude $\left(\approx 10^{-5}\right)$, which indicates that GQD doping does not introduce interface defects within the cell. The ideality factor γ remains in the $[1;2]$ range for GQD doped samples, which means that QD-DSSC devices still exhibit diode behavior. Furthermore, the fill-factor FF is increased with 0.17 for the sample doped with 1 mg GQD,

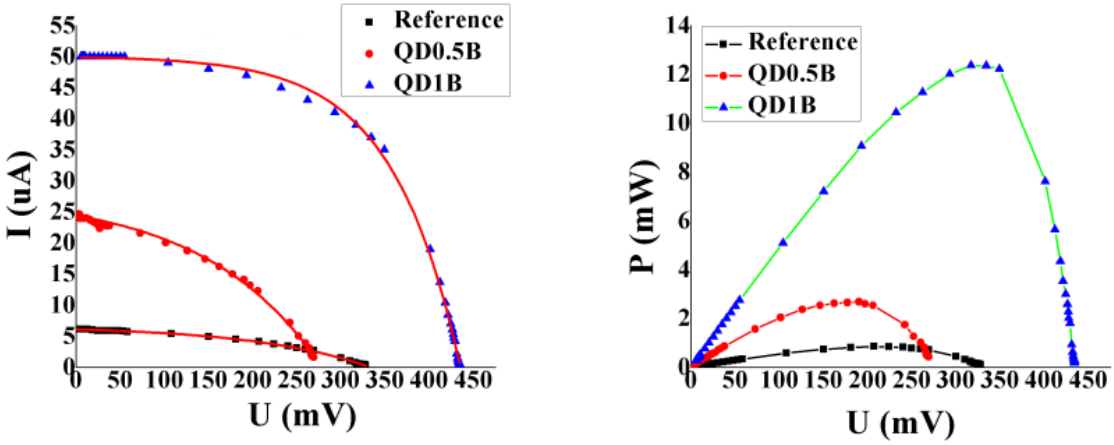

Fig. 6. IV and PV curves obtained for DSSC samples QD0.5A and QD1A, respectively, under halogen lamp illumination

Sample code	U_{oc} (mV)	I_{sc} (μA)	R_p $(k\Omega)$	R_s (Ω)	γ	P_{max} (μW)	FF	η $(\%)$
Reference	328	6.13	150	$1.35 \cdot 10^{-5}$	1.56	0.85	0.42	1.70
QD0.5B	269	24.6	20	$8.44 \cdot 10^{-5}$	1.19	2.68	0.40	5.36
QD1B	434	50	7500	$2.95 \cdot 10^{-5}$	2.00	12.40	0.57	11.27

TABLE 1. Numerical values of device parameters for the studied DSSC-QD samples, where U_{oc} - open-circuit voltage, I_{sc} - short-circuit current, R_p - cell shunt resistance, R_s - cell series resistance, γ - cell ideality factor, P_{max} - cell maximum power yield, FF - fill-factor, η - power-conversion efficiency

which indicates that GQD doping improves device IV curve form. Most importantly, power-conversion efficiency η reaches 11.27% for the sample doped with 1 mg GQD, compared to the 1.70% efficiency yielded by the reference sample. These preliminary results indicate a potential of DSSC performance optimization through quantum dot doping, without the danger of introducing device defects, and by preserving the device's diode behavior.

5. Conclusions

This paper presents a novel method for ruthenium DSSC device optimization through graphene quantum-dot doping. The TiO_2 cathodes are doped with various masses of graphene quantum dots, by treatment with a water-based solution containing graphene quantum dot suspensions. A DSSC sample doped with 1 mg graphene quantum dots yielded a 11.27% power-conversion efficiency, which represents a difference of 9.57%, compared to a 1.70% efficiency obtained with a undoped reference ruthenium DSSC sample. Device parameter values obtained for the quantum-dot treated sample also indicate that the process of doping does not insert bulk or interface defects within the device, and preserves its diode-like behavior.

REFERENCES

[1] *M. Gratzel*, Dye-sensitized solar cells, J. Photochem. Photobiol. C **4**(2), 145 – 153 (2003).

[2] *S. Sathyajothi , R. Jayavel and A. Clara Dhanemozhi*, The fabrication of natural dye sensitized solar cell (dssc) based on tio2 using henna and beetroot dye extracts, Materials Today: Proceedings **4**(2, Part A), 668 – 676 (2017).

[3] *G. Richhariya , A. Kumar , P. Tekasakul and B. Gupta*, Natural dyes for dye sensitized solar cell: A review, Renew. Sustain. Energy Rev **69**, 705 – 718 (2017).

[4] *B. O'Regan and M. Gratzel*, A low-cost, high-efficiency solar cell based on dye-sensitized colloidal tio2 films, Nature **353** (1991).

[5] *S. R. Raga and F. Fabregat-Santiago*, Temperature effects in dye-sensitized solar cells, Phys. Chem. Chem. Phys. **15**, 2328 – 2336 (2013).

[6] *A. Barar, M. Vladescu and P. Schiopu*, Effect of temperature on the parameters of a bulk heterojunction organic solar cell, Acta Tehnica Napocensis-Electronics and Telecommunications **59** (2018).

[7] *A. Barar, D. Manaila-Maximean, C. Boscornea, M. Vladescu and P. Schiopu*, Thermal behavior of the electrical parameters for a novel zinc derivative-based dye-sensitized solar cell, Proc. of SPIE **10977** (2019).

[8] *A. Mishra, M. K. R. Fischer and P. Bauerle*, Metal-free organic dyes for dye-sensitized solar cells: from structure: property relationships to design rules, Angew. Chem., Int. Ed. **48** (2009).

[9] *V. Aranyos, J. Hjelm, A. Hagfeldt and H. Grennberg*, Free-base tetra-arylphthalocyanines for dye-sensitised nanostructured solar cell applications, J. Porphyrins and Phthalocyanines **5** (2001).

[10] *M. K. Nazeeruddin, A. Kay, I. Rodicio, R. Humphry-Baker, E. Mueller, P. Liska, N. Vlachopoulos and M. Gratzel*, Conversion of light to electricity by cis-x2bis(2,2'-bipyridyl-4,4'-dicarboxylate)ruthenium(ii) charge-transfer sensitizers (x = cl-, br-, i-, cn-, and scn-) on nanocrystalline titanium dioxide electrodes, J. Am. Chem. **115** (1993).

[11] *M. K. Nazeeruddin, P. Pechy and M. Gratzel*, Efficient panchromatic sensitization of nanocrystalline tio2 films by a black dye based on a trithiocyanato–ruthenium complex, Chem. Commun. (1997).

[12] *M. K. Nazeeruddin, M. K. Zakeeruddin, R. Humphry-Baker, R. Jirousek, P. Liska, N. Vlachopoulos, V. Schklover, C. H. Fischer and M. Gratzel*, Acid−base equilibria of (2,2'-bipyridyl-4,4'-dicarboxylic acid)ruthenium(ii) complexes and the effect of protonation on charge-transfer sensitization of nanocrystalline titania, Innorg. Chem. **38** (1999).

[13] *H. Sugihara, L. P. Singh, K. Sayama, H. Arakawa, M. K. Nazeeruddin and M. Gratzel*, Efficient photosensitization of nanocrystalline tio2 films by a new class of sensitizer: cis-dithiocyanato bis(4,7-dicarboxy-1,10-phenanthroline)ruthenium(ii), Chem. Lett. **27** (1998).

[14] *A. Hagfeldt, G. Boschloo, L. Sun, L. Kloo, and H. Pettersson*, Dye-sensitized solar cells, Chem. Rev. **110** (2010).

[15] *J. Gong, K. Sumathy, Q. Qiao and Z. Zhou*, Review on dye-sensitized solar cells (dsscs): Advanced techniques and research trends, Renew. Sustain. Energy Rev **68** (2017).

[16] *K. Sharma, V. Sharma and S. S. Sharma*, Dye-sensitized solar cells: Fundamentals and current status, Nanoscale Res. Lett **13** (2018).

[17] *F. Gao, Y. Wang, J. Zhang, D. Shi, M. Wang, R. Humphry-Baker, P. Wang, S. M. Zakeeruddin and M. Gratzel*, A new heteroleptic ruthenium sensitizer enhances the absorptivity of mesoporous titania film for a high efficiency dye-sensitized solar cell, Chem. Comm. **23** (2008).

[18] *O.Danila*, Spectroscopic assesment of a simple hybrid si-au cell metasurface-based sensor in the mid-infrared domain, J. Quant. Spectr. Rad. Trans. **254**(107209) (2020).

[19] *A. Barar, O. Danila and P. Schiopu*, Generation of continuous polarization distribution in a single laser beam, U. P. B. Sci. Bull. **81**(2) (2019).

[20] *E. Petrescu, C. Cirtoaje and O. Danila*, Dynamic behavior of nematic liquid crystal mixtures with quantum dots in electric fields, Beilstein J. Nanotech. **9**(1) (2018).

[21] *D. Manaila-Maximean, O. Danila, P. L. Almeida, and C. P. Ganea*, Electrical properties of a liquid crystal dispersed in an electrospun cellulose acetate network, Beilstein. J. Nanotech **9**(1) (2018).

[22] *D. Manaila-Maximean, O. Danila, C. Cirtoaje and D. Donescu*, Novel colloidal system: magnetite-polymer particles/lyotropic liquid crystal under magnetic field, J. Magn. Mag. Mat. **438** (2017).

[23] *O. Danila and P. Sterian*, Entanglement manifestation in laser structures, Rom. Rep. Phys. **67**(3) (2015).

[24] *J. Shen, Y. Zhu, C. Chen, X. Yang, and C. Li*, Facile preparation and upconversion luminescence of graphene quantum dots, Chem. Comm. **9** (2010).

[25] *M. Bacon, S. J. Bradley and T. Nann*, Graphene quantum dots, Part. Part. Syst. Charact. **31** (2013).
[26] "Am 1.5 solar emission spectrum." `https://www.nrel.gov/solar_radiation/` (2010).
[27] *S. P. Singh, K. S. V. Gupta, G. D. Sharma, A. Islam and L. Han*, Efficient thiocyanate-free sensitizer: a viable alternative to n719 dye for dye-sensitized solar cells, Dalton Trans. **41** (2012).
[28] *P. Wen, Y. Han and W. Zhao*, Influence of tio2 nanocrystals fabricating dye-sensitized solar cell on the absorption spectra of n719 sensitizer, Int. J. Photoenergy **2012** (2012).
[29] *A. Barar, D. Manaila-Maximean, M. Vladescu and P. Schiopu*, Simulation of charge carrier transport mechanisms for quantum dot-sensitized solar cells, U. P. B. Sci. Bull. Series A **88** (2019).
[30] *A. A. Mohammed, A. S. S. Ahmad and W. A. Azeez*, Fabrication of dye-sensitized solar cell based on titanium dioxide (tio2), Adv. Mater. Phys. Chem. **5** (2015).
[31] *A. Barar, O. Danila, D. Manaila-Maximean and M. Vladescu*, Parameter extraction of an organic solar cell using asymptotic estimation and lambert w function, Proc. of SPIE **10010**(1001034) (2016).
[32] *A. Barar, M. Vladescu and P. Schiopu*, Theoretical characterization of polymer-bulk heterojunction organic solar cells, U. P. B. Sci. Bull. Series A **80** (2018).
[33] *G. del Pozo, B. Romero and B. Arrendondo*, Extraction of circuital parameters of organic solar cells using the exact solution based on lambert w-function, Proc. of SPIE **8435** (2012).
[34] *A. Jain and A. Kapoor*, A new approach to study organic solar celll using lambert w-function, Sol. Energy Mater. Sol. Cells **86**, 197–205 (2005).